Estimate of Loads During Wing-Vortex Interactions by Munk's Transverse-Flow Method

Vernon J. Rossow*
NASA Ames Research Center, Moffett Field, California 94035

The inviscid, incompressible interaction of a wing with a vortex is studied by use of Munk's transverse-flow method. The method assumes that the loading on the wing is such that the local circulatory flow of the vortex is turned so that the wing and its vortex wake act as a barrier to the flow. This permits the analysis to be carried out by mapping the transverse flowfield into the flow about a circle to find the vorticity distribution in the wake. Closed-form expressions are then derived for the bound circulation in the wing and for the lift and rolling moment induced by the vortex on the encountering wing. Comparisons of the loads predicted by these relationships with those of vortex-lattice theory for a flat wing of a rectangular planform indicate that they accurately represent the various parameters when the aspect ratio of the encountering wing is less than about two. When flat rectangular wings of higher aspect ratios are considered, some sort of correction is needed. Examples are then presented to illustrate some applications of the results.

Nomenclature

$\mathcal{R}$ = aspect ratio
a = radius of circle in mapped plane
b = wing span
C_L = lift coefficient, $=L/qS$
C_l = rolling-moment coefficient, $=M/Sb$
c = wing chord
L = lift
M = rolling moment
q = dynamic pressure, $=\rho U_\infty^2/2$
r = radius
S = wing planform area
U_∞ = velocity of aircraft
w = vertical velocity
x = distance in flight direction
y = distance in spanwise direction
z = distance in vertical direction
γ = wake vorticity
Γ = bound circulation of wing
ζ = complex variable, $=y+iz$
θ = meridian angle
ρ = air density
Φ = complex potential

Subscripts

c = circle plane
f = following or probe aircraft
g = wake-generating aircraft
im = image vortex
m = maximum
o = centerline of following wing
s = slit plane
v = vortex

Received Feb. 2, 1989; revision received Aug. 1, 1989.

*Senior Scientist. Associate Fellow AIAA.

Introduction

IN a number of aerodynamic problems,[1-9] the flowfields contain the interaction of a vortex with a wing, rotor blade, or aircraft surface. Since such a flowfield is complex and contains large velocity gradients, it is often necessary to approximate various aspects of the fluid motion in order to facilitate a solution. The present study began as a part of the NASA program to find ways to alleviate[1-6] the overturning velocities that now exist in the lift-generated wakes of large transport aircraft. The analyses used in that research often require simple and accurate means for calculating the interaction of a wing with a vortex to estimate the rolling moment induced on a small aircraft following a larger wake-generating aircraft. In the past, some effort and thought has gone into the definition and justification of various theoretical approaches to the wing-vortex interaction.[1-21] A review of this information[6] indicates that further analysis is required to define better the interaction of the vortex with an aerodynamic surface. In particular, improved resolution is needed in those cases wherein the vortex impinges near or right on the leading edge of a wing because the interaction may substantially modify the distribution of velocity in the vortex.

Once the far-field structure of the vortex is known from experiment or from a theoretical estimate, one of several methods can presently be chosen to estimate the loading. If the vortex-lattice method[16] is chosen to analyze the flowfield, the flow-angularity impressed on the aerodynamic surfaces by the vortex is interpreted as the local angle of attack of the wing surface to a uniform freestream. This step reformulates the mixed (rotational and potential) flowfield into one that is approximated by potential flow. That is, the original flowfield, which is composed of a flat wing submerged in the rotating flowfield of a vortex, is replaced by a twisted wing in a uniform airstream. Such a change in the character of the flowfield raises questions as to the quality of the results and has prompted discussion[8-21] of concerns and of possible remedies. The region of most concern occurs when the high speed core of the vortex is near a surface so that the angles of attack induced on the wing are large enough to be out of the linear range assumed in the approximations. That is, high rotational velocities in the core region of the vortex impress large angles of attack on the nearby aerodynamic surfaces. If this concentration of vorticity is not redistributed by the interaction process,

unrealistically large loads are predicted. Since the radius of the vortex is usually not large in high speed cores, the momentum in the fluid is small. The large loads predicted are then not supported by the large mass flux of fluid that is assumed in the twisted wing approach[6] currently used in the vortex-lattice and strip-theory methods.

The present investigation was undertaken primarily in response to a continuing need for improved methods by which wakes can be compared with one another to determine their level of hazard for following aircraft. In particular, theoretical wakes being considered for wake alleviation[6] are often composed of a system of point or line vortices which have cores of zero diameter and infinite velocities at their centers. Use of the usual strip theories or vortex-lattice methods in these situations yields unrealistic results if the center of a vortex is too near a control point. The solutions presented here yield realistic results for all types of interactions with simple, closed-form expressions for the various flowfield parameters. After the flowfield and its idealizations are described, the steps used to obtain a solution are presented along with several applications of the results. Not only do the present results provide a simple solution to a complicated problem, but they also provide a step toward a more complete analysis, which better represents the true nature of the flowfield. The present solutions can also be used for comparison with numerical results to test their validity.

Description of Flowfield

The problem being considered here (Fig. 1) assumes that the axis of the vortex is aligned with the flight direction of the wing. The vortex is assumed to have a circulation of Γ_v and to be positive when it has counterclockwise rotation from a pilot's viewpoint. The vortex is located at a distance r_{sv} from the centerline of the wing at an elevation angle of θ_{sv} relative to the spanwise direction of the wing. The surface that encounters the vortex is shown as a rectangular wing for simplicity, but the analysis treats the wing as a lifting line and does not specify its shape. It is simply assumed that the wing planform, camber, and twist are constructed so that the lift distribution at each spanwise station is just enough to turn the swirling fluid of the vortex so that it does not penetrate the wing or the wake. It is also assumed that the wake trailing from the lifting line remains as a flat sheet and does not roll up or undergo any self-induced distortions. Since the wing and its wake form a barrier to the fluid motion of the vortex, the analysis treats the wake as a flat surface that is not penetrated by the fluid. The procedure used to obtain the solutions presented here is patterned after the transverse-flow method described in Chap. V of Munk,[10] wherein the flow about the wake is considered as two dimensional to determine the vorticity distribution in the wake. Munk used this method to derive elliptic loading as the most efficient for a given span and to analyze other lifting systems. Since a slender-body assumption is not made, the shape of the wing and any change in cross section with streamwise distance is not included (e.g., Chap. II of Munk[10]).

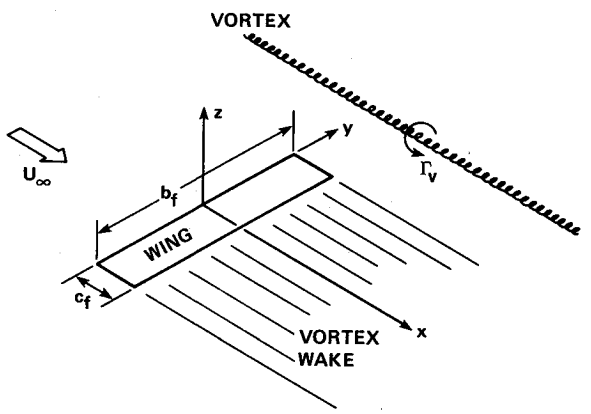

Fig. 1 Schematic of flowfield.

Analysis

Since the wake shed by the encountering wing is assumed to remain as a flat, impermeable sheet from the wing trailing edge to infinity, the flowfield far downstream of the wing in a plane transverse to the flight direction (and vortex axis) can be treated as two dimensional.[10] If the vortex wake is taken to be a slit of vanishingly small separation between the upper and lower surfaces (Fig. 2), it can be mapped from a circle by the function

$$\zeta_s = \zeta_c + a^2/\zeta_c \tag{1}$$

or

$$y_s = y_c(1 + a^2/r_c^2) \tag{2a}$$

$$z_s = z_c(1 - a^2/r_c^2) \tag{2b}$$

where $y_c = r_c \cos\theta_c$, $z_c = r_c \sin\theta_c$, and $r_c^2 = y_c^2 + z_c^2$. Unfortunately, Eqs. (2a) and (2b) are simple when mapping from the circle to the slit plane but not so when going in the other direction, which happens to be the one necessary in the present analysis. Several attempts were first made to invert Eqs. (1) and (2), but they all result in unmanageable expressions which became ambiguous when the mapping did not involve the first quadrant. Further difficulty also arose in these expressions when the signs of multiple-valued square roots had to be chosen. A very satisfactory scheme was then found by first squaring both Eqs. (2a) and (2b) and then combining the results in such a way as to eliminate the dependence on θ_c. As a result, a quadratic equation was generated for the quantity, $(r_c^2 + a^4/r_c^2)$, as

$$(r_c^2 + a^4/r_c^2)^2 - r_s^2(r_c^2 + a^4/r_c^2) - 2a^2(2a^2 - y_s^2 + z_s^2) = 0 \tag{3}$$

Solution of Eq. (3) for the quantity inside the parentheses yields another quadratic equation in terms of r_c^2, which is again easily solved. The quantity r_c is then found by taking the square root obtained from the solution of the second quadratic equation. In each of these steps, the positive sign is chosen for the square root to be sure that r_c^2 remains positive. After r_c has been found, θ_c is found by use of Eqs. (2a) and (2b). In the computations for the mapping, a point on or just outside of the circle or slit is always taken slightly in excess of the circle radius (i.e., above or below the slit that represents the wake) to be certain that the point in question is in the flowfield and not inside the circle or slit.

Since the flowfield is linear, the contributions of any number of vortices can be superimposed. For the present, however, consider a single vortex passing somewhere near a wing and its wake as shown in Figs. 1 and 2. If the circle in the mapped plane is to be a boundary, an image vortex must be placed inside the circle at the same angle θ_{cv} as the impinging vortex and at the radius $r_{im} = a^2/r_{cv}$ from the center of the circle. An additional vortex of the same strength as the impinging vortex

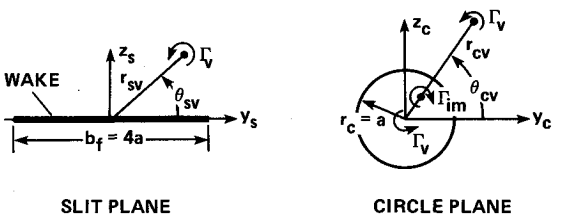

Fig. 2 Illustration of mapping of slit in physical plane that contains vortex wake shed by encountering wing from a circle by use of the relationship $\zeta_s = \zeta_c + a^2/\zeta_c$.

must be placed at the center of the circle so that the net circulation inside the circle and, therefore, in the wake vanishes. Since both a positive and negative vortex are added to the flowfield, the net circulation upstream and far downstream of the wing are both equal to the magnitude of the circulation in the impinging vortex. If a vortex had not been added at the center of the circle, the net or total circulation in the transverse flowfield far downstream of the wing would be zero. The complex potential for the cross-stream flowfield is then given by

$$\Phi = (i\Gamma_v/2\pi)\,\ell n[\zeta_c(\zeta_c - \zeta_{cv})/(\zeta_c - a^2/\bar{\zeta}_{cv})] \tag{4}$$

where no tangency or Kutta condition is specified at the edges of the wake. The solution given by Eq. (4) yields the potential and stream function when separated into real and imaginary parts. The velocity components are found by taking the complex derivative of Eq. (4). The velocity on the surface of the slit is then found from the circumferential velocity on the surface of the circle as

$$v_s = (v_c \sin\theta_c - w_c \cos\theta_c)/2 \sin\theta_c \tag{5}$$

The vorticity in the wake is found from

$$\gamma_s(y_s) = v_s)_{\text{lower}} - v_s)_{\text{upper}} \tag{6}$$

Substitution of the various derived quantities into Eq. (6) yields the vorticity distribution for the wake in terms of the wing span b_f or the radius of the circle, $a = b_f/4$ and the location of the impinging vortex in the circle plane as

$$\gamma(y_s) = \left(\frac{\Gamma_v}{4\pi a \sin\theta_c}\right)\left[2 - \frac{r_{cv}^2 - a^2}{r_{cv}^2 + a^2 - 2ar_{cv}^2 \cos(\theta_c - \theta_{cv})} - \frac{r_{cv}^2 - a^2}{r_{cv}^2 + a^2 - 2ar_{cv}^2 \cos(\theta_c + \theta_{cv})}\right] \tag{7}$$

where a position on the slit is related to a corresponding one on the circle by

$$y_s = 2a \cos\theta_c \tag{8}$$

The span loading on the encountering or following wing is obtained by integration[22] of the intensity of the vortex wake $\gamma_s(y_s)$ for the bound circulation $\Gamma(y_s)$ or

$$\Gamma(y_s) = -\int_{-b_f/2}^{y_s} \gamma(y)\,dy$$

to yield

$$\Gamma(y_s) = -\left(\frac{\Gamma_v}{\pi}\right)\left\{\theta_c - \tan^{-1}\left[\frac{(r_{cv}+a)}{(r_{cv}-a)}\tan[(\theta_c - \theta_{cv})/2]\right] - \tan^{-1}\left[\frac{(r_{cv}+a)}{(r_{cv}-a)}\tan[(\theta_c + \theta_{cv})/2]\right]\right\} \tag{9}$$

When Eq. (9) is used to compute the span loading, the arc tangents sometimes switch quadrants at improper values of the arguments so that the loading contains errors and unwanted discontinuities. This difficulty can be eliminated by combining the two arc tangent functions through the use of trigonometric identities so that Eq. (9) becomes

$$\Gamma(y_s) = -\left(\frac{\Gamma_v}{\pi}\right)\left\{\theta_c - \tan^{-1}\left[\frac{(r_{cv}^2 + a^2)\sin\theta_c}{(r_{cv}^2 + a^2)\cos\theta_c - 2ar_{cv}\cos\theta_{cv}}\right]\right\} \tag{10}$$

Now that the circulation bound in the wing is known, the lift and torque induced on the wing by the vortex can be found by integration of the equations

$$L = -\rho U_\infty \int_{-b_f/2}^{b_f/2} \Gamma(y_s)\,dy_s \tag{11a}$$

$$M = -\rho U_\infty \int_{-b_f/2}^{b_f/2} y_s \Gamma(y_s)\,dy_s \tag{11b}$$

The integrations are carried out by first transforming them to the circle plane. Integration by parts is then used to conform the integrals to fit those listed in the integral tables of Dwight.[22] By this technique, the coefficients of lift and rolling moment induced on the following or encountering wing by a vortex are found as

$$C_{Lf} = -\mathcal{R}_f(\Gamma_v/b_g U_\infty)(b_g/b_f)(a/r_{cv})\cos\theta_{cv} \tag{12}$$

$$C_{lf} = -[\mathcal{R}_f/8](\Gamma_v/b_g U_\infty)(b_g/b_f)(a^2/r_{cv}^2)\cos 2\theta_{cv} \tag{13}$$

where a positive value of lift is taken as upward and a positive value of rolling moment as one in the same direction as the impinging vortex. An equation for the drag due to lift that corresponds to Eqs. (12) and (13) was not derived because the integrations were not obvious.

The dependence of the induced lift and rolling moment on span ratio, aspect ratio, and the strength and location of the vortex relative to the wing centerline is defined by Eqs. (12) and (13). It should be noted that Eqs. (4–10) are given in terms of the location of the vortex in the circle plane even though the quantities represented apply to the slit or physical plane. Transformation back and forth between the two planes is relatively easy by use of Eqs. (2) and (3).

Results similar to Eqs. (12) and (13) are presented in Nielsen (pp. 101 and 107).[8] When those results are changed into the present notation, they become

$$C_{Lf} = -\mathcal{R}_f(\Gamma_v/b_g U_\infty)(b_g/b_f)[1 - (a/r_{cv})^2]\cos\theta_{cv}$$

$$C_{lf} = -[\mathcal{R}_f/8](\Gamma_v/b_g U_\infty)(b_g/b_f)[1 + (a/r_{cv})^2]\cos\theta_{cv}$$

Nielsen's equations also predict a side force on the wing, whereas the present method indicates that it is zero. The difference in the two results is not surprising because the method of analysis is different and Nielsen's result for rolling moment is for a wing of triangular planform. (Wing planform can be included if the slender-body approximation is made.) An application[9] of Nielsen's method was outlined for a wing of rectangular planform with a nearby vortex whose path was allowed to vary with chordwise distance. Since the integrals then became quite messy, the analysis could not be carried to the completion presented here.

Some intuitive insight into the physics of the lift and moment are obtained by changing Eqs. (12) and (13) into another form. First recognize that $\cos\theta_{cv} = y_{cv}/r_{cv}$, $\cos 2\theta_{cv} = (y_{cv}^2 - z_{cv}^2)/r_{cv}^2$, and that the vertical velocity at the center of the circle that represents the wing wake in the mapped plane is given by $w_o = -(\Gamma_v/2\pi)(y_{cv}/r_{cv}^2)$. Hence, Eqs. (12) and (13) may be written as

$$C_{Lf} = [\pi\mathcal{R}_f/2](w_o/U_\infty) \tag{14}$$

$$C_{lf} = [\pi\mathcal{R}_f/64](b_f/U_\infty)\,dw_o/dy_o \tag{15}$$

where dw_o/dy_o is the gradient of the vertical velocity at the center of the circle. Even though it has been known for some time that the lift and torque induced on a wing by a vortex were, respectively, proportional to the vertical velocity and its lateral gradient, it was not known that the relationship was exact when those quantities were evaluated in the circle plane. These relationships are not any improvement over Eqs. (12) and (13) because their evaluation is the same, but they provide

insight into the nature of the lift and torque imposed on an encountering wing by nearby vortices.

Comparison with Other Methods

The solutions derived by Munk's transverse-flow method are now examined not only to illustrate the character of the predictions but also to find out how well they compare with the loads induced on a flat wing of rectangular planform. Since the shape of the wing is not specified by the theory, there is some question as to how the results presented here should be tested. If the wing is cambered and/or twisted to redirect the rotary flow of the impinging vortex, the results could be made to agree exactly because the assumptions would be the same. However, a different wing shape must then be used for each vortex strength and location. It seems best then to compare the present predictions on the basis of a flat wing of rectangular planform which does not fit any aircraft in particular but is representative of most wing shapes in use. The methods available[6] to be used as a reference in the comparison range from quite simple strip-theory-type analyses to fairly involved finite-difference methods. Of these, the two methods to be used here are a modified strip theory, which incorporates features suggested by Munk, Jones, and Maskew,[6] and a vortex-lattice method developed by Hough.[16] Both methods assume that the wake is not changing with time and that the penetrating wing is fixed at some point in the wake so that the flowfield can be treated as steady state. The differences between these two prediction schemes for the maximum torque on a following wing were found to be small compared with the uncertainties usually experienced in obtaining test data.[6,9,20–24] Since the span-load distribution predicted by strip theory is directly proportional to the local upwash without any redistribution of vorticity, it is not useful for comparison with the load or vorticity distributions. Hence, the modified strip theory will be used only to derive equations for the lift and torque induced on the wing when the vortex is at its most effective location for each quantity, and the vortex-lattice method will be used to make more detailed comparisons.

The first of the two quantities to be derived with the modified strip theory is the lift induced on an encountering wing when the vortex impinges on the wing at a distance y_v from the wing centerline. Since the impinging vortex is a potential vortex and has no core, the velocity distribution is given by

$$v_\theta = \Gamma_v/2\pi r \tag{16}$$

Integration of the lift distribution when the vortex is in the $z=0$ plane yields

$$C_{Lf})_{\text{strip}} = [1/(1+3/\mathcal{R}_f)](\Gamma_v/b_g U_\infty) \times (b_g/b_f)\ln[(y_v - b_f/2)/(y_v + b_f/2)] \tag{17}$$

where the aspect ratio function inside the first set of brackets arises from the empirical correction for strip theory suggested by Jones and Cohen.[12]

Similarly, the rolling moment induced by the vortex on the encountering wing is found by integration of the torque to yield

$$C_{lf})_{\text{strip}} = [1/(1+6/\mathcal{R}_f)](\Gamma_v/b_g U_\infty)(b_g/b_f) \times \{1 + 0.5\ln[(y_v - b_f/2)/(y_v + b_f/2)]\} \tag{18a}$$

The empirical aspect-ratio function of Jones and Cohen differs slightly from Eq. (17) to Eq. (18a) to reflect the fact that the maximum torque location for the vortex puts half of the wing in an upwash and half in a downwash flowfield making the effective aspect ratio half as large as when the vortex impinges at the wingtip.[6,10] Note that both Eqs. (17) and (18a) become infinite when the vortex impinges on either wingtip; i.e., $y_v = \pm b_f/2$. This characteristic makes it difficult to use

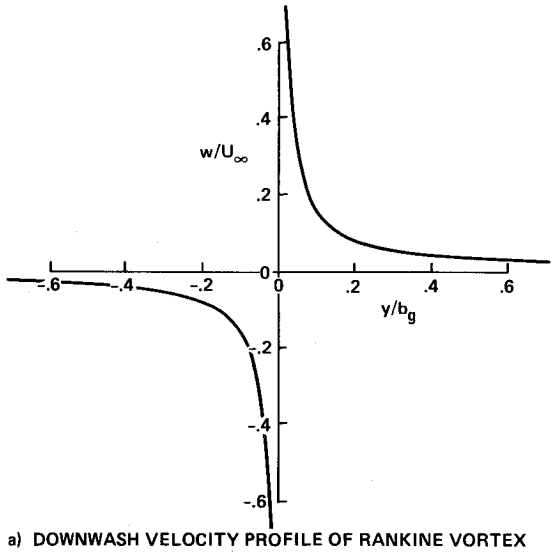

a) DOWNWASH VELOCITY PROFILE OF RANKINE VORTEX USED TO APPROXIMATE A POINT VORTEX; $r_{core}/b_g = 0.001$, $\Gamma_v/b_g U_\infty = 0.1$

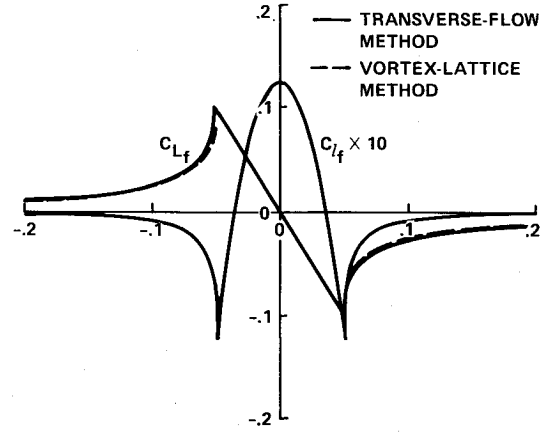

b) LIFT AND ROLLING MOMENT; $\Gamma_v/b_g U_\infty = 0.1$, $b_f/b_g = 0.5$, $AR_f = 1$

Fig. 3 Variation of lift and rolling-moment coefficients with spanwise distance along a line just above the vortex center.

these equations for flowfields that contain point or line vortices because the answer may depend on the proximity of a vortex to a control point. Vortex-lattice methods present a similar difficulty whenever a point vortex falls on or too near a control point and, therefore, are also not useful for flowfields that contain point vortices. When the vortex impinges on the wing centerline, the lift vanishes and the rolling-moment coefficient takes on a finite value.

$$C_{lf})_{\text{strip}} = [1/(1+6/\mathcal{R}_f)](\Gamma_v/b_g U_\infty)(b_g/b_f) \tag{18b}$$

The maximum values predicted by the transverse-flow method for lift and rolling moment are given by Eqs. (12) and (13) as

$$C_{Lf})_m = \mathcal{R}_f(\Gamma_v/b_g U_\infty)(b_g/b_f) \tag{19}$$

$$C_{lf})_m = [\mathcal{R}_f/8](\Gamma_v/b_g U_\infty)(b_g/b_f) \tag{20}$$

It is to be noted that the strip theory result, Eq. (18b), has the same form except for the aspect ratio function. It is for this reason that in each of these equations, the dependency on $\mathcal{R}_f$ is indicated by square brackets to emphasize where the functional difference between various theories appears to be concentrated. Since the strip theory result for maximum rolling

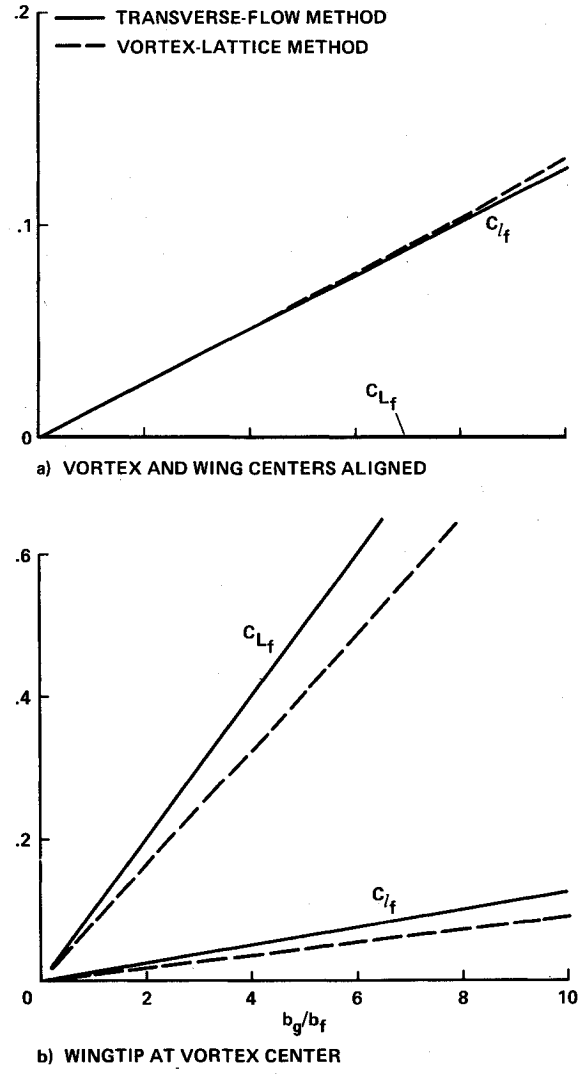

Fig. 4 Variation of lift and rolling-moment coefficients with the inverse of the span ratio of the generating and following wing as predicted by transverse-flow and vortex-lattice methods; $\Gamma_v/b_g U_\infty = 0.1$, $\mathcal{R}_f = 1$.

moment and vortex-lattice theory have been found to be in good agreement with experiment,[24] the results obtained with the transverse-flow method need to be examined in more detail to find out how well they compare with the loads on flat wings of rectangular planform.

The vortex-lattice method[16] makes possible an evaluation of the accuracy of the transverse-flow predictions for the vortex-induced span loadings and the integrated parameters. Since the vortex-lattice method is a numerical procedure, the velocity distribution of the vortex must not contain infinite values in case a control point inadvertently falls on or near the center of vortex. In order to cover such a possibility and still have a vortex structure that approximates a potential vortex, the vortex used in the comparisons was a Rankine vortex[23] with a small but finite core of radius, $r_{core} = 0.001 b_f$ (part a of Fig. 3). Even though a small core is specified for the vortex, the vortex-lattice solution responds as if the core were as large as the distance to the control point nearest the center of the vortex. Such an approximation does not always affect the results significantly but may be responsible for some of the differences between the two predictions. The wing used for the vortex-lattice computation has a rectangular planform and has no twist or camber. The span and chord are adjusted to achieve the desired values of $\mathcal{R}_f$ and b_g/b_f.

As expected, all of the expressions derived for the wing-vortex interaction indicate a linear relationship with the dimensionless vortex strength. Such a relationship is expected in the absence of flow separation or other flow anomalies that lead to nonlinear characteristics. Such a well-behaved linear characteristic for the other parameters like the span ratio b_g/b_f and the aspect ratio of the following wing $\mathcal{R}_f$ is not necessarily expected. Hence, these variations will now be investigated.

The lift and rolling moment predicted by the transverse-flow method and the vortex-lattice method are first compared in Fig. 3 as the wing is given locations along a line just above the horizontal axis of the vortex. As mentioned in the preceding discussion, the vortex used in the vortex-lattice computation was given a core of radius of $r_{core} = 0.001 b_f$ (part a of Fig. 3). Even with this precaution, unrealistically large positive and negative values of lift and rolling moment occurred at locations along the y axis between $y_v = -0.5 b_f$ and $+0.5 b_f$ whenever the vortex center was too near a control point of a wing panel or lattice. For this reason, a dashed curve for the vortex-lattice prediction is not presented in Fig. 3 over that range of y values. Outside of this region, no portion of the wing is near the vortex center so the vortex-lattice method does not have difficulty, and the two predictions are in good agreement.

The span ratio parameter b_g/b_f was chosen as the next part of Eqs. (12) and (13) to be studied because all of the equations predict a linear dependence of lift and torque on it. The comparison in part a of Fig. 4 indicates that the relationship is indeed not only linear but the rolling moments are in very good agreement when the vortex center and the wing centerline are aligned. However, when the vortex impinges on the wingtip, the agreement is not as good, even though the transverse-flow and vortex-lattice methods both predict a linear relationship with b_g/b_f. The reason for the lack of agreement is not obvious but, as mentioned previously, may be caused by the dependence of the vortex-lattice method on the nearness of the control points to the vortex center. The finite mesh size of the vortex-lattice method may also contribute to the difference but not significantly.

Next the effect of aspect ratio on the lift and rolling moment predicted by the two methods are compared (Fig. 5). Once again, the quantities are evaluated at the vortex locations that yield maximum values for each. As observed in Fig. 3, the lift has a maximum whenever a wingtip is at the vortex center. The magnitude of the rolling moment maximum predicted by the transverse-flow method is the same at the wingtips as at the wing centerline [Eq. (13)]. The comparisons in Fig. 5 show that the linear relationship predicted by the transverse-flow method is not confirmed by the vortex-lattice results. As anticipated by the assumptions made in the transverse-flow theory, the two predictions are in agreement with one another at low values of $\mathcal{R}_f$. As $\mathcal{R}_f$ increases, however, the transverse-flow method increasingly overpredicts the loading. Such a result points out that the encountering wing needs a large chord if, as assumed in the theory, the wing is to turn the rotary flowfield of the vortex so that it does not penetrate the wake. Hence, even though the theory of the transverse-flow method did not specify the planform of the wing or its twist and camber, it did require that the wing should be of a size and shape that would deflect the rotating airstream around the wake. As indicated in Fig. 5, one possible design that accomplishes the flow diversion is a wing with a large chord or small aspect ratio. According to the results of the comparison, the required amount of turning is apparently provided by the flat rectangular wing used in the vortex-lattice examples when its aspect ratio is below about one.

It was thought for awhile that the transverse-flow result could be corrected by a simple aspect-ratio function similar to the Jones and Cohen[12] empirical formula and perhaps the same as the one given in Eq. (17) or (18). Trial-and-error attempts were then used to develop a function of $\mathcal{R}_f$ that would bring the two predictions into agreement. A function

that corrects for lift when the vortex is aligned with a wingtip is given by

$$F_L(\mathcal{R}_f) = [1 + 0.5\mathcal{R}_f^{0.32}] \tan(0.6\mathcal{R}_f) \quad (21a)$$

A function that corrects the rolling moment prediction when the vortex is aligned with the wing centerline is given by

$$F_l(\mathcal{R}_f) = [1 + 1.6\mathcal{R}_f^{0.29}] \tan(0.4\mathcal{R}_f) \quad (21b)$$

If Eqs. (21a) and (21b) are used instead of the simple $\mathcal{R}_f$ parameter in Eqs. (19) and (20), the straight lines presented in Fig. 4 for the transverse-flow method are converted into curved lines that lie within a line width of the vortex-lattice results. However, when Eqs. (21a) and (21b) were applied to other locations of the vortex relative to the wing to obtain the span loading, lift, and rolling moment, the agreement with vortex-lattice theory was not nearly as good. Some of the lack of agreement may be because of failures of the vortex-lattice method to represent some aspects of the aerodynamic interaction process. However, most of the difference probably occurs because the transverse-flow result assumes that the following wing (no matter what its shape) turns the rotary flow so that it does not penetrate the wing or the wake, whereas the vortex-lattice theory assumes only that the wing itself is not penetrated by the vortex flowfield. When both predictive methods are applied in circumstances where their respective assumptions are not violated, the two results agree. In the cases considered, they agree well only when the aspect ratio is small.

In order to illustrate further the character of the transverse-flow results, the span loadings are compared with vortex-lattice results in Fig. 6 for $\mathcal{R}_f = 1$ when the vortex is aligned with the wing centerline and with the wingtip. Once again the vortex center is not near enough to a vortex-lattice control point to yield unrealistic results, but the loading may also not be accurately represented. Note that the agreement is quite good except for the lift magnitude when the vortex impinges on the wingtip. Such a difference is expected when the comparisons in Fig. 5 are examined at low values of $\mathcal{R}_f$. Other comparisons made in the study suggest that a separate aspect ratio function will probably be needed for each wing shape and vortex location to achieve a high degree of accuracy.

Applications

Several examples of the kinds of problems that can be treated by use of the results of the transverse-flow method [Eqs. (12) and (13)] are now presented to illustrate applications. The author's primary interest was to have available a simple, quick means for the calculation of the contours of constant lift and torque for any system of point vortices, e.g., one that represents a lift-generated wake. In order to illustrate such a capability, the contours for a single or isolated vortex are first presented in Fig. 7. Such a computation is relatively simple because they are known in closed form from Eqs. (12) and (13).

In the case of two or more vortices, a predictor/corrector method is used to generate the contours. The contours for a pair of point vortices are presented in Fig. 8 for both lift and rolling moment in order to illustrate application to the simplest of lift-generated wakes.

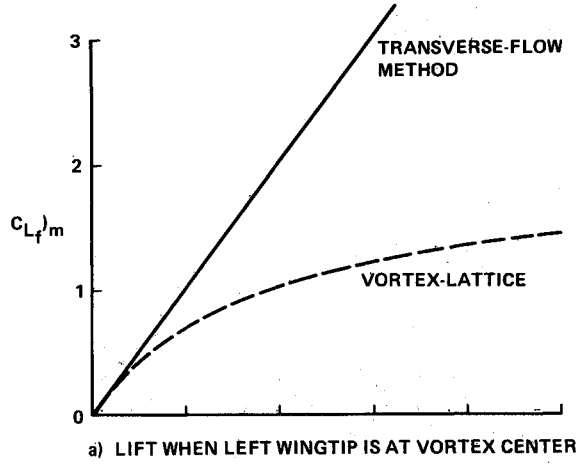

Fig. 5 Variation of lift and rolling moment coefficients with aspect ratio of the following wing as predicted by transverse-flow and vortex-lattice methods; $\Gamma_v/b_g U_\infty = 0.1$, $b_f/b_g = 0.2$.

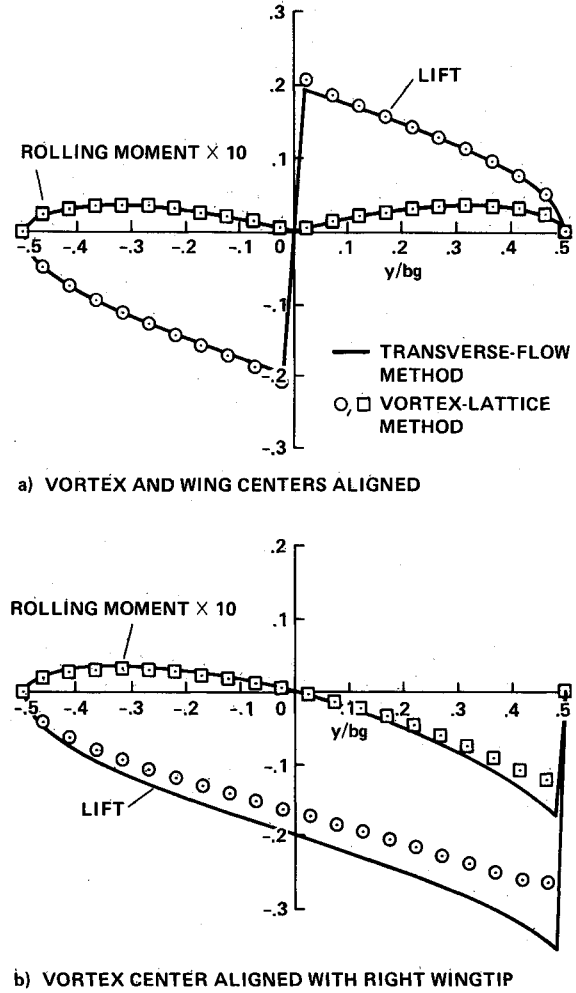

Fig. 6 Comparison of spanwise loading as predicted by the transverse-flow and vortex-lattice methods; $\Gamma_v/b_g U_\infty = 0.1$, $b_f/b_g = 0.5$, $\mathcal{R}_f = 1$.

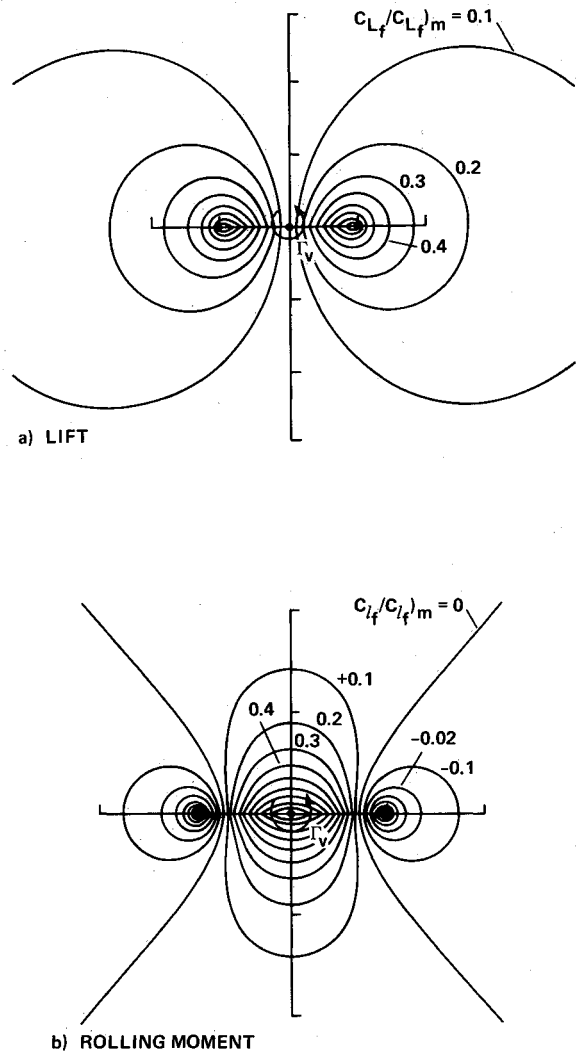

Fig. 7 Predictions by transverse-flow method of the contours of equal lift and rolling moment coefficients as induced on a following wing by a point vortex.

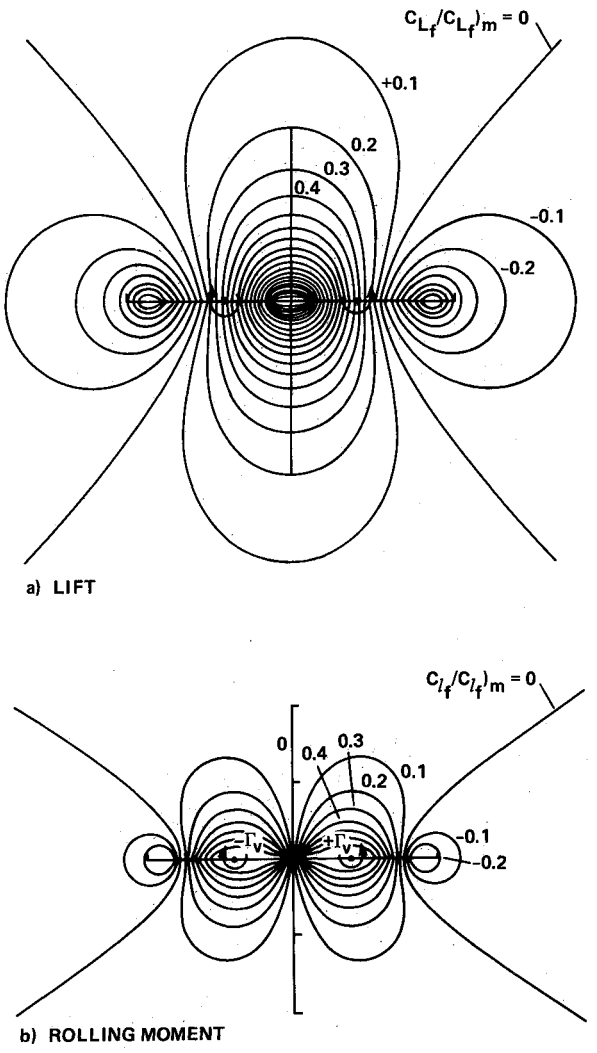

Fig. 8 Predictions by transverse-flow method of the contours of equal lift and rolling moment coefficients as induced on a following wing by a vortex pair; $b_f/b_g = 1$.

Obviously, these results are easily extended by superposition to any number and arrangement of point vortices which thereby provides the tools sought at the beginning of the investigation. In order to illustrate the technique and to check the accuracy of the approximation of vortex structure by a number of point vortices, an example is presented in Fig. 9. In the case presented, the structure of the vortex core of a Rankine vortex is simulated with 19-point vortices. Comparison is then made with the vortex-lattice method by assuming a continuous distribution of velocity in the vortex so that the computation does not have difficulty. In order to indicate the accuracy of the point vortex approximation, the two predictions are compared in Fig. 9 along a line through the center of the vortical region. Since the agreement is quite good, the example illustrates the effectiveness with which a system of point vortices can be used to represent a continuous distribution of vorticity. The wiggles in the transverse-flow prediction are small-scale versions of the fluctuations shown in Fig. 3 for a single vortex. As the number of vortices used to simulate a given vortex structure increases, the amplitude the length of the wiggles decreases.

Another example which illustrates the use of Eqs. (12) and (13) for estimating lift and torque throughout a vortex wake is presented in Fig. 10. A system of 40-point vortices is used to represent the lift-generated wake of an elliptically loaded wing. The contours of constant torque are presented at several time intervals or distances downstream of the wing trailing edge as noted in the figure. The technique developed to produce Fig. 10 makes it possible to evaluate the wake hazard as a function of time for a wide variety of lifting configurations. In the cases studied so far, it was found that the maximum rolling moment induced on a following wing by a vortex system does not change appreciably during the time history of the wake even though the contours change somewhat. This result is not expected to be true for all wakes because the maximum value of the gradient in vertical velocity is not an invariant of vortex systems. It should also be noted that the maximum torque predicted is larger than any of those measured in wind tunnels for two reasons. First, viscous effects diffuse the high energy concentrated in the vortex cores. Second, most of the wakes measured were shed by wings with slats and flaps which again tend to diffuse the cores of vortices and reduce the induced torque.

In all of these examples, note that, even though wiggles occur in the contours due to the finite number of point vortices used in the simulation, the predicted torque does not take on unrealistic values as the vortex impinges on any part of the encountering wing. This attribute makes the foregoing results useable in a variety of circumstances not possible with strip or vortex-lattice theories unless special precautions are taken to avoid the proximity of vortex center to control points. If the aspect ratio of the following wing is to be much greater than one, an empirical adjustment, such as Eq. (21), should be

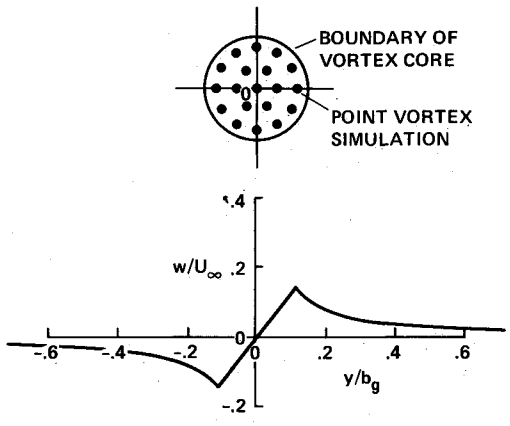

a) DOWNWASH THROUGH CENTER OF RANKINE VORTEX AND ILLUSTRATION OF ITS POINT VORTEX SIMULATION; $r_{core} = b_f$

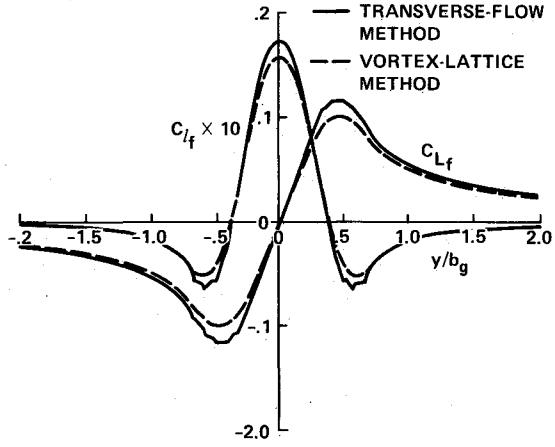

b) COMPARISON OF PREDICTIONS ALONG A LINE JUST ABOVE THE VORTEX CENTER

Fig. 9 Lift and rolling moment on a wing as it traverses through vortex with a core of radius $r_{core} = b_f$. Transverse-flow method uses a system of point vortices that simulate the continuous distribution of vorticity of the Rankine vortex used in the vortex-lattice method; $b_f/b_g = 0.5$, $\mathcal{R}_f = 1.0$, $\Gamma_v/b_gU_\infty = 0.1$.

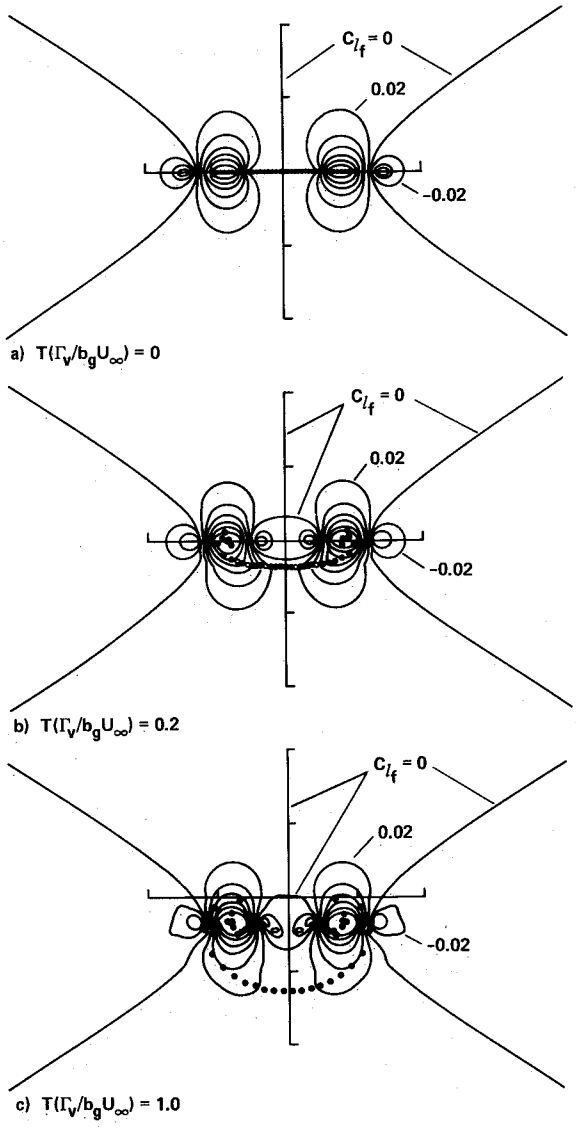

Fig. 10 Contours of equal rolling moment coefficient at various instants of time as the wake shed by an elliptically loaded wing rolls up; $\Gamma_v/b_gU_\infty = 1$, $b_f/b_g = 0.5$, $\mathcal{R}_f = 1$, rolling moment increment between contours = $\Delta C_{lf}/(\Gamma_v/b_gU_\infty) = 0.02$; $C_{lf})_m/(\Gamma_v/b_gU_\infty) = 0.175$.

made to the results predicted by the transverse-flow method to improve the quantitative accuracy of the method for aspect ratios much above one.

One other use for the simple closed-form lift and rolling moment expressions is in the use of ground-based simulators to study the interaction of aircraft with vortex wakes and the corresponding response of the pilots to the encounter.[6,25] In simulations of this kind, strip theory was usually used to estimate the induced loads in order to achieve a computation time sufficiently small that the aircraft response time and the simulation could be realistic. Use of the foregoing closed-form equations for the lift and torque for the various surfaces on the aircraft would facilitate the computation.

Concluding Remarks

The interaction of a vortex with a wing has been analyzed by use of Munk's transverse flow method which assumes that the wing and its wake are a barrier to the rotary flowfield of the vortex. Such an idealization simplifies the analysis so that simple closed-form expressions are derived for the loads induced on the following wing. The analysis is explicit with regard to boundary condition and the subsequent loadings, but no specification is made on the wing shape. As a consequence, the predicted results are in agreement with vortex-lattice theory for a flat wing of rectangular planform when it has a chord long enough (i.e., aspect ratio less than about two) to turn the local rotary flow of the vortex as assumed in the transverse-flow theory. At larger aspect ratios, the closed-form results diverge from the vortex-lattice predictions for flat rectangular wings.

These comparisons add confidence in the vortex-lattice method's ability to properly represent rearrangement of the velocity and vorticity in complicated flowfields. The comparisons also demonstrate that the closed-form expressions derived by Munk's transverse flowfield method are quantitatively correct at small aspect ratios and qualitatively correct elsewhere. A correction at higher values of $\mathcal{R}_f$ for the fact that the wing under consideration does not turn the flow of the vortex as completely as assumed in the theory was found for the lift and rolling moment at vortex locations that yield maximum values of each. Unfortunately, application of these corrections to other vortex/wing locations provides improved but questionable accuracy because the correction is a function of not only aspect ratio but also of the vortex location relative to the wing.

The closed-form results derived herein have a number of applications where a simple description is useful. An easy method for the evaluation of the lift and rolling moment im-

posed on encountering wings by various lift-generated wakes will enhance the development of lifting systems that have alleviated wakes. Application to the blade/vortex interaction in helicopter research and to the simulation of aircraft entering a vortical flowfield are also possible applications.

References

[1]Olsen, J. H., Goldburg, A., and Rogers, M., (eds.), *Aircraft Wake Turbulence and its Detection,* Plenum, New York, 1971.

[2]Hallock, J. N., "Aircraft Wake Vortices—An Annotated Bibliography (1923–1975)," U.S. Dept. of Transportation, Rept. FAA-RD-76-43, Jan. 1976.

[3]NASA Symposium on Wake Vortex Minimization, NASA SP-409, 1976.

[4]Hallock, J. N., (ed.), *Proceedings of the Aircraft Wake Vortices Conference,* U.S. Dept. of Transportation, Rept. FAA-RD-77-68, March 1977.

[5]Wood, W. D., (ed.), *FAA/NASA Proceedings Workshop on Wake Vortex Alleviation and Avoidance,* U.S. Dept. of Transportation, Rept. FAA-RD-79-105, Nov. 1978.

[6]Rossow, V. J., and Tinling, B. E., "Research on Aircraft/Vortex-Wake Interactions to Determine Acceptable Level of Wake Intensity," *Journal of Aircraft,* Vol. 25, No. 4, June 1988, pp. 481–492.

[7]Widnall, S., "Helicopter Noise Due to Blade-Vortex Interaction," *Journal of the Acoustical Society of America,* Vol. 50, No. 1, Pt. 2, July 1970, pp. 354–365.

[8]Nielsen, J. N., *Missile Aerodynamics,* McGraw-Hill, New York, 1960, pp. 101–107.

[9]McMillan, O. J., Schwind, R. G., Nielsen, J. N., and Dillenius, M. F. E., "Rolling Moments in a Trailing Vortex Flow Field," NASA CR-151961, Feb. 1977.

[10]Munk, M. M., *Fundamentals of Fluid Dynamics for Aircraft Designers,* Ronald Press, New York, 1929.

[11]Heaslet, M. A. and Spreiter, J. R., "Reciprocity Relations in Aerodynamics," NACA Rept. 1119, 1953.

[12]Jones, R. T., and Cohen, D., "Aerodynamics of Wings at High Speeds," *High Speed Aerodynamics and Jet Propulsion—Aerodynamic Components of Aircraft at High Speeds,* Vol. VII, edited by A. F. Donovan and H. R. Lawrence, Princeton University Press, Princeton, NJ, 1957.

[13]Jones, W. P., "Vortex-Elliptic Wing Interaction," *AIAA Journal,* Vol. 10, Feb. 1972, pp. 225–227.

[14]Filotas, L. T., "Vortex Induced Wing Loads," *AIAA Journal,* Vol. 10, July 1972, pp. 971.

[15]Maskew, B., "Numerical Lifting Surface Methods for Calculating the Potential Flow about Wings and Wing-Bodies of Arbitrary Geometry," Ph.D. Thesis, Loughborough Univ. of Technology, Loughborough, England, UK, Oct. 1972.

[16]Hough, G., "Remarks on Vortex-Lattice Methods," *Journal of Aircraft,* Vol. 10, May 1973, pp. 314–317.

[17]Barrows, T. M., "Simplified Methods of Predicting Aircraft Rolling Moments Due to Vortex Encounters," *Journal of Aircraft,* Vol. 14, May 1977, pp. 434–439.

[18]Flax, A. H., "Comment on Simplified Methods of Predicting Aircraft Rolling Moments Due to Vortex Encounters," *Journal of Aircraft,* Vol. 14, Nov. 1977, pp. 1151–1152.

[19]Barrows, T. M., "Reply to A. H. Flax," *Journal of Aircraft,* Vol. 14, Nov. 1977, p. 1152.

[20]McMillan, O. J., Nielsen, J. N., Schwind, R. G., and Dillenius, M. F. E., "Rolling Moments in a Trailing-Vortex Flow Field," *Journal of Aircraft,* Vol. 15, May 1978, pp. 280–286.

[21]Holbrook, G. T., "Vortex Wake Hazard Analysis Including the Effect of the Encountering Wing on the Vortex," M. S. Thesis, George Washington Univ., Washington, DC, Aug. 1985.

[22]Dwight, H. B., *Tables of Integrals and Other Mathematical Data,* 4th ed., MacMillan, New York, 1964, p. 105.

[23]Lamb, H., *Hydrodynamics,* 6th ed., Dover, New York, 1945, Chaps. 11, 12.

[24]Rossow, V. J., Corsiglia, V. R., Schwind, R. G., Frick, J. K. D., and Lemmer, O. J., "Velocity and Rolling-Moment Measurements in the Wake of a Swept-Wing Model in the 40- by 80-Foot Wind Tunnel," NASA TM X-62,414, April 1975.

[25]Sammonds, R. I., and Stinnett, G. W., Jr., "Hazard Criteria for Wake Vortex Encounters," NASA TM X-62,473, Aug. 1975.